Electric Form Factor of the Neutron

Shigeyuki Tajima
田嶋　重行

University of Virginia

Outline

- Introduction
- Electromagnetic Form Factors
- Unpolarized Techniques to extract Gen
- Double-Polarization Techniques
  - E93-038 (Recoil Polarimetry)
  - E93-026 (Polarized deuteron target)
  - E02-013 (Polarized 3He target)
- Summary

Motivations for G_{En} Experiment

- Precise knowledge of the nucleon form factors is needed for understanding the electromagnetic structure of the nucleons.
- Values of the nucleon form factors are used for testing nucleon models.
- The electric form factor of the neutron, G_{En} is not well known at high Q^2 (>2 (GeV/c)^2).

Historical Background (I)
(Structure of the nucleon)

	Predicted values if they *were* point particles	Measured Values	Anomalous Values
Proton	1.0	2.79	1.79
Neutron	0.0	-1.91	-1.91

Magnetic moments of the proton and neutron in units of nuclear magneton, $\mu_N = \frac{e\hbar}{2M_p}$

e : Electron charge magnitude

M_p : Proton mass

Historical Background (II)

(Structure of the nucleon)

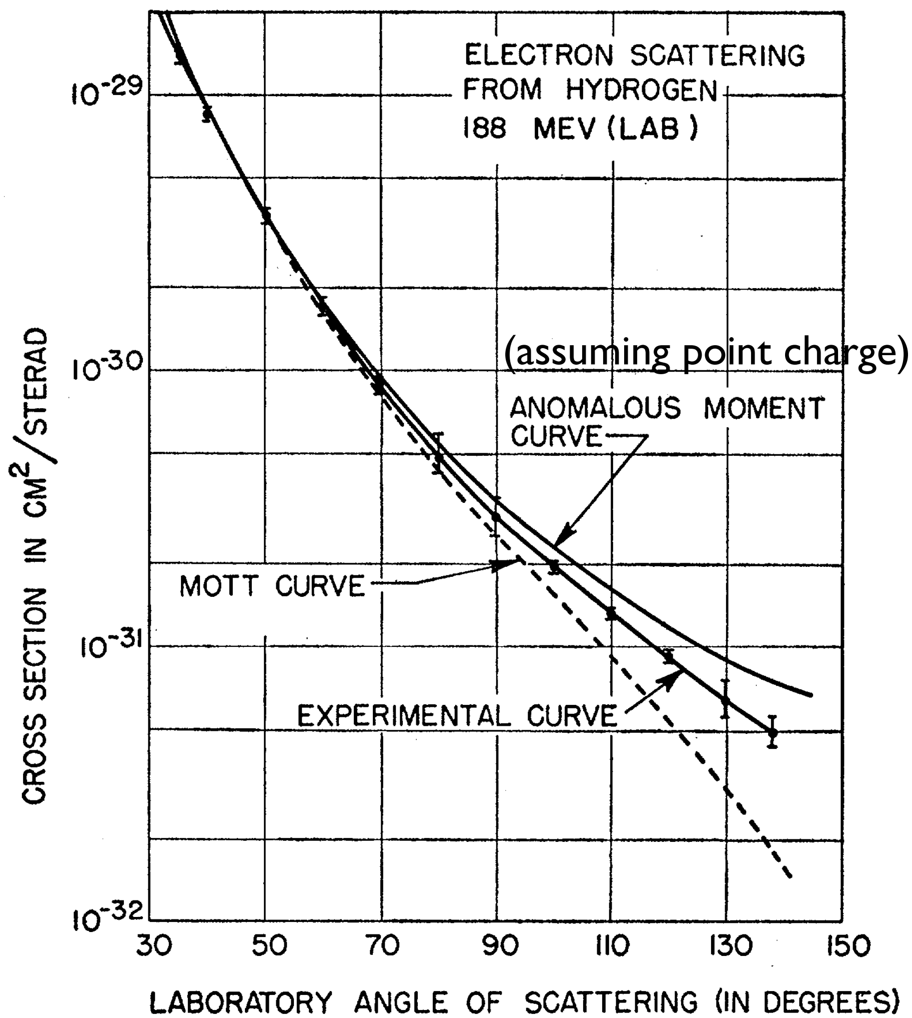

- Elastic electron scattering from proton by R.Hofstadter (1955)
- The measured cross section does not follow the theoretical curve which assumes no internal structure.
  - This indicates that the proton possesses an internal structure.

Electromagnetic Form Factors

- Nucleon EM Form Factors: G_{Ep}, G_{Mp}, G_{En}, G_{Mn}
- In the non-relativistic limit, Ge and Gm are related to charge and magnetic moment distribution inside nucleon.
- Magnetic form factors are well measured
  (G_{Mp} measured to Q^2~30 $(GeV/c)^2$)
- G_{En} is difficult to measure and very poorly known!!
  (*Precise* measurements of G_{En} are performed to Q^2 ~1.5 $(GeV/c)^2$)

G_E^n World data (Q^2<2(GeV/c)^2)

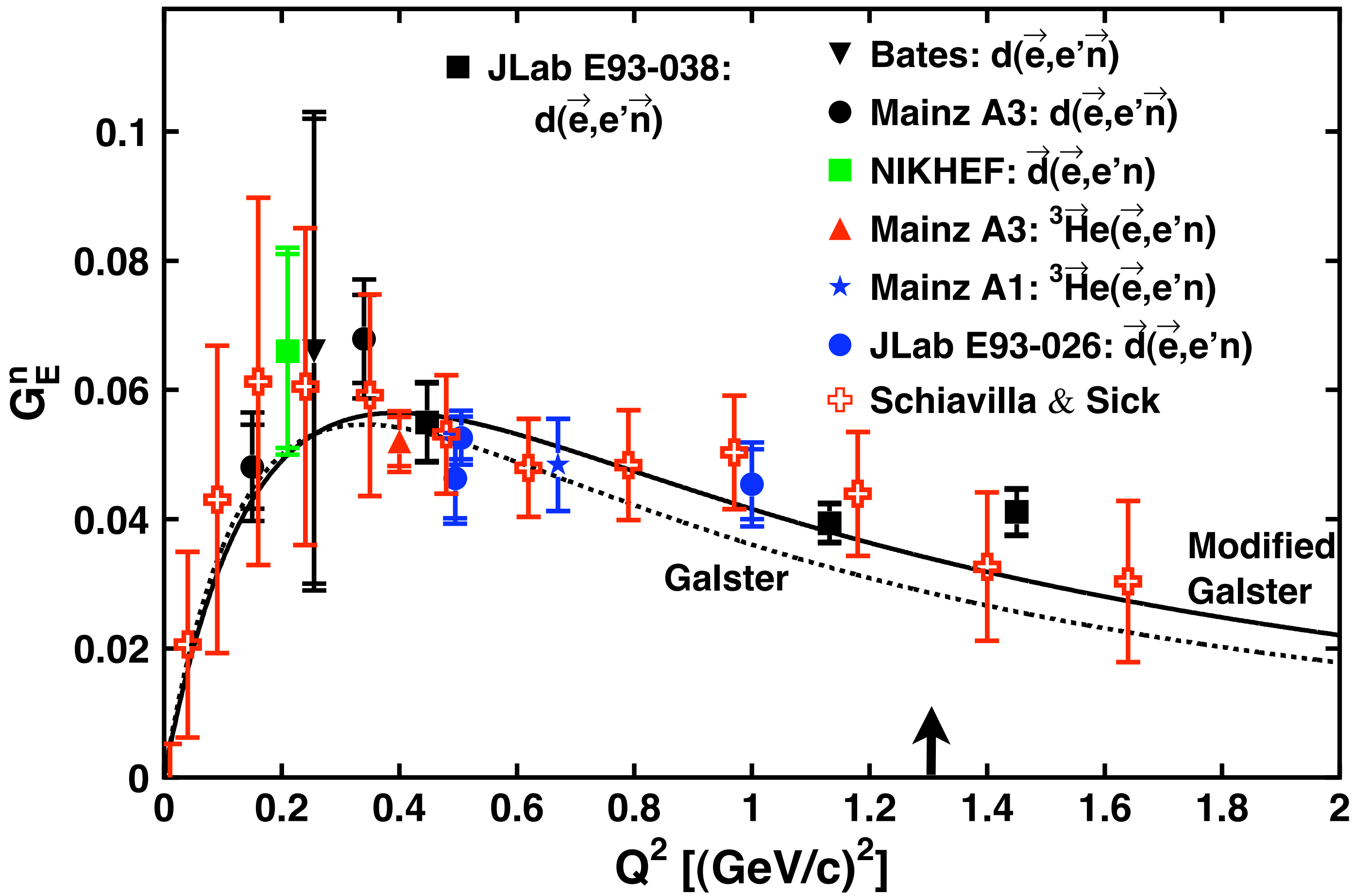

All but Schiavilla&Sick data are obtained using double-polarization technique

G_E^n World data (High Q^2)

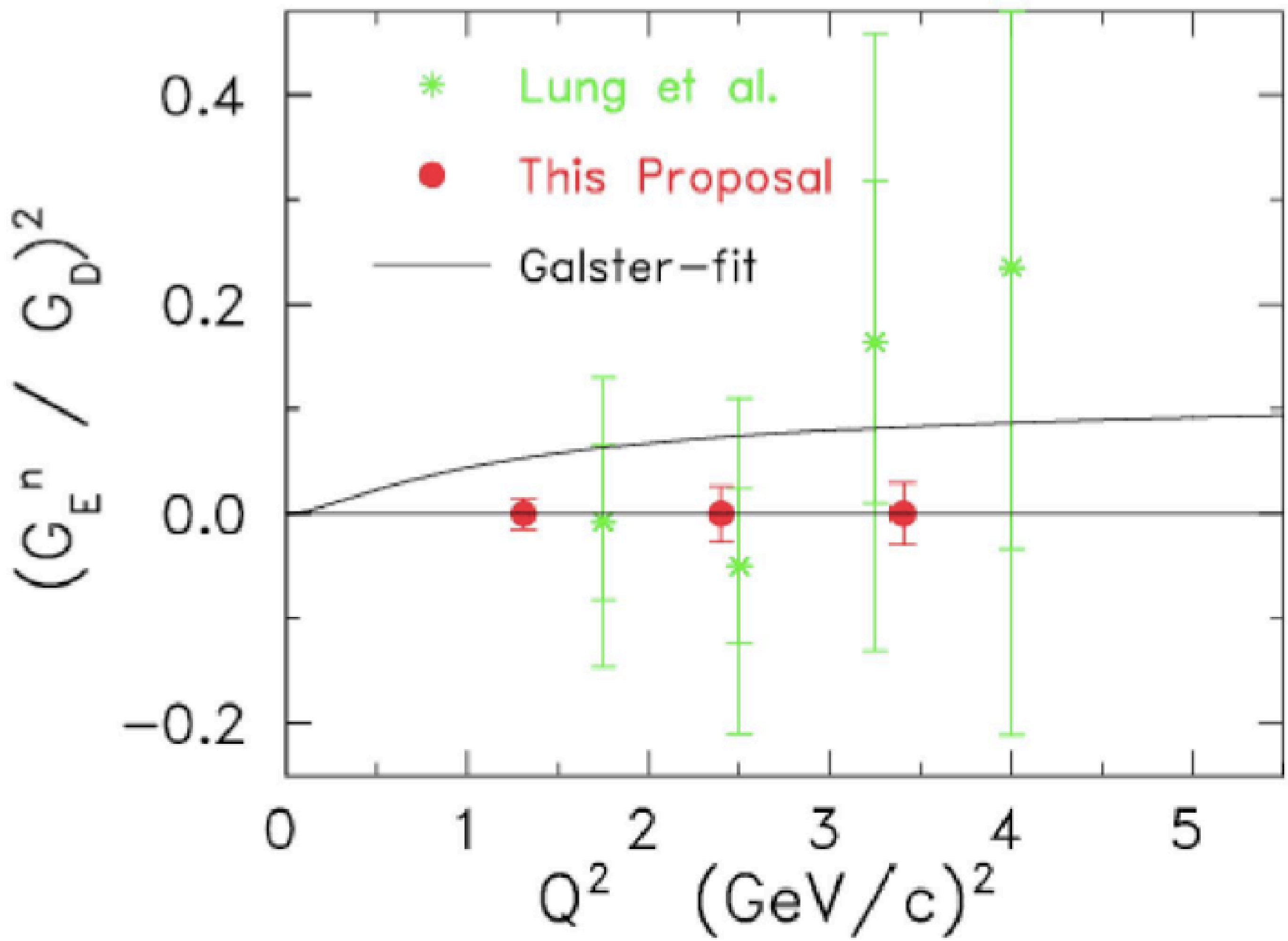

G_M^n World Data

(The magnetic form factor of the neutron)

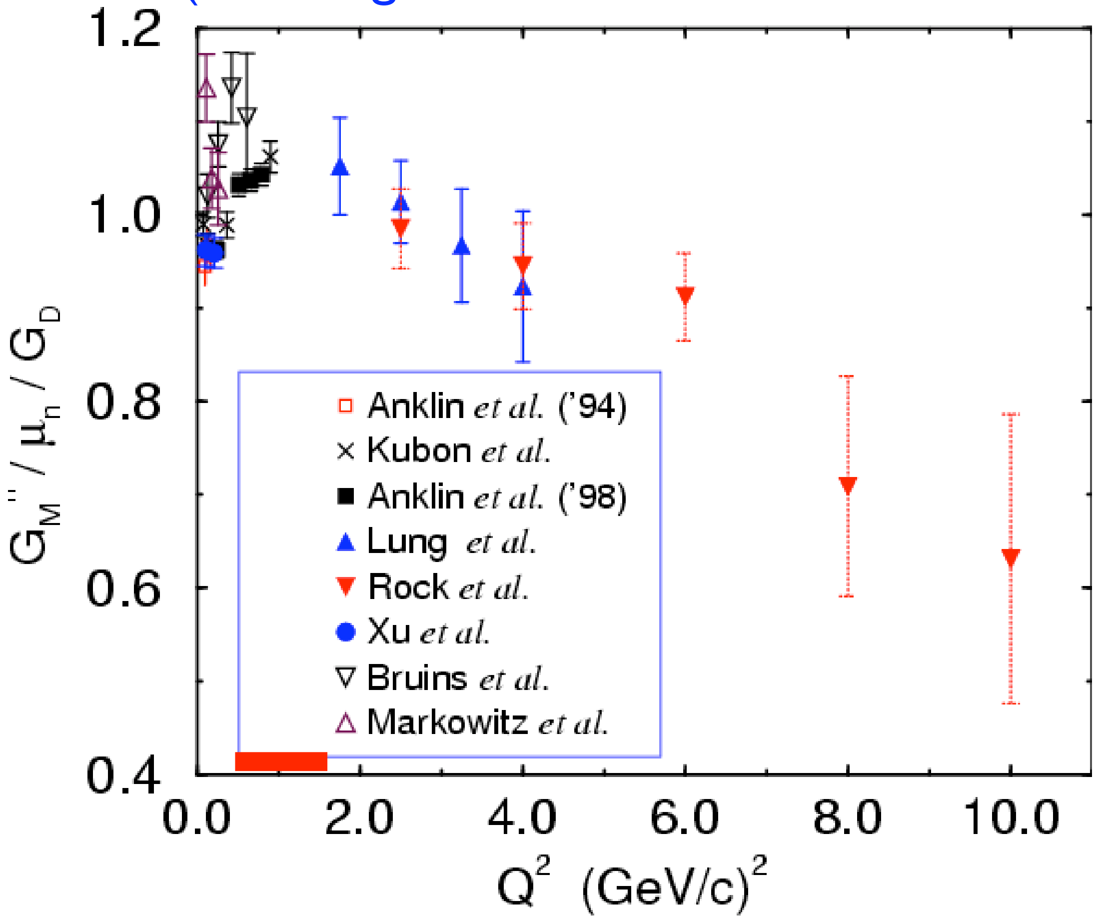

The value of G_M^n is needed for a determination of G_E^n from G_{En} / G_{Mn}

➡ G_M^n from a fit to the world data can be used.

Electron scattering from a spin ½ finite particle

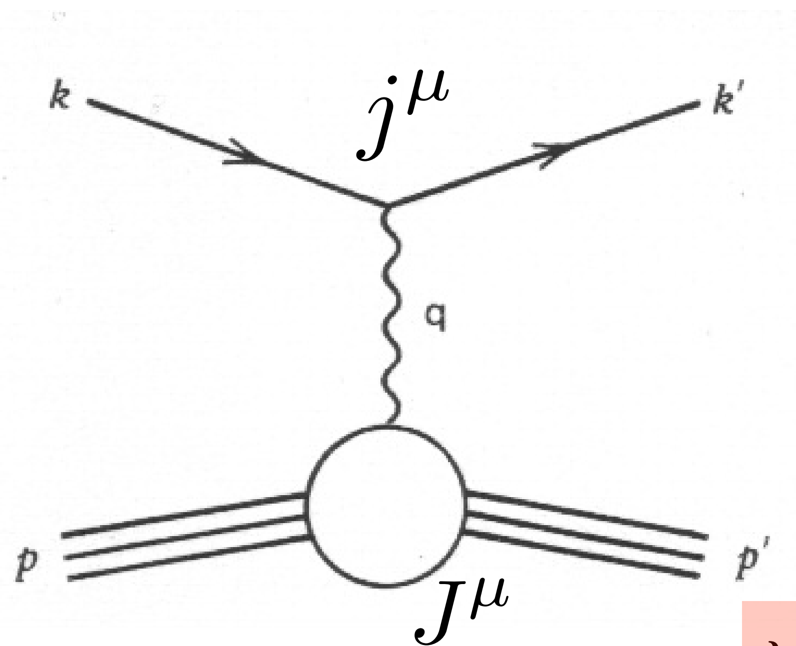

$$T_{fi} = -i \int j_\mu \left(\frac{-1}{q^2}\right) J^\mu d^4x$$

EM currents:

$$j_\mu = -e\,\bar{u}(k')\,\gamma^\mu\,u(k)\,e^{i(k'-k)\cdot x}$$

$$J^\mu = e\,\bar{u}(p')\,\lambda^\mu\,u(p)\,e^{i(p'-p)\cdot x}$$

$$\lambda^\mu = F_1(q^2)\,\gamma^\mu + \frac{\kappa}{2M} F_2(q^2)\,i\,\sigma^{\mu\nu} q_\nu$$

- q^2 : Four-momentum transfer squared
- F_1 and F_2 are Dirac and Pauli Form Factors.

Probing the Structure of Nucleons

Electron scattering from a spin ½ point particle

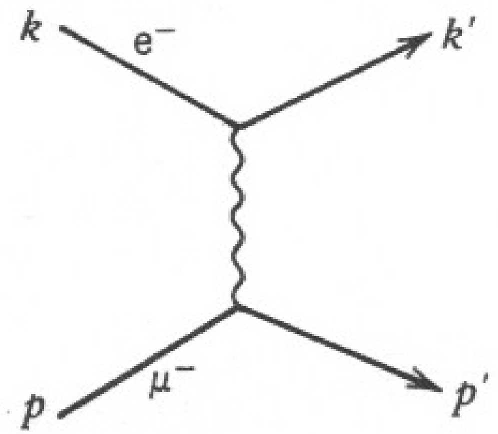

$$\left.\frac{d\sigma}{d\Omega}\right|_{\text{lab.}} = \left(\frac{\alpha^2}{4E^2\sin^4\frac{\theta}{2}}\right)\frac{E'}{E}\left\{\cos^2\frac{\theta}{2} - \frac{q^2}{2M^2}\sin^2\frac{\theta}{2}\right\}$$

E Incident electron energy

E' Scattered electron energy

Probing the Structure of Nucleons

Electron scattering from a spin ½ point particle

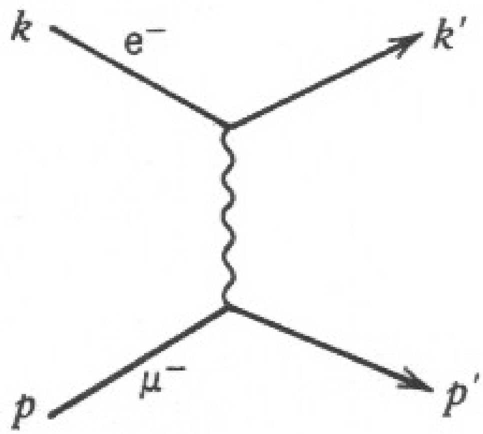

$$\left.\frac{d\sigma}{d\Omega}\right|_{\text{lab.}} = \left(\frac{\alpha^2}{4E^2\sin^4\frac{\theta}{2}}\right)\frac{E'}{E}\left\{\cos^2\frac{\theta}{2} - \frac{q^2}{2M^2}\sin^2\frac{\theta}{2}\right\}$$

E Incident electron energy

E' Scattered electron energy

Electron scattering from a spin ½ finite particle

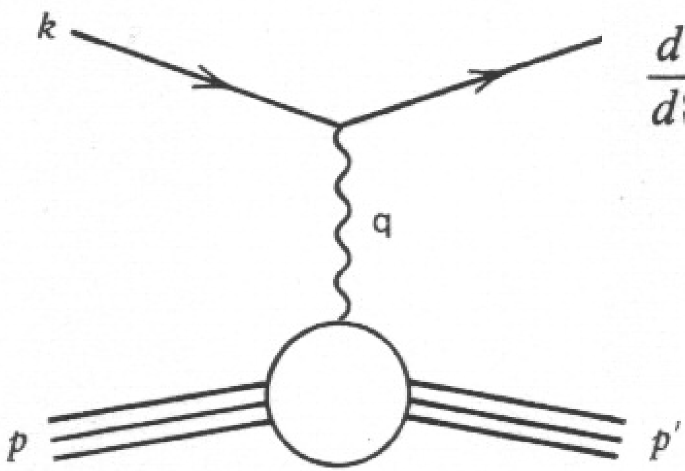

$$\left.\frac{d\sigma}{d\Omega}\right|_{\text{lab}} = \left(\frac{\alpha^2}{4E^2\sin^4\frac{\theta}{2}}\right)\frac{E'}{E}\left\{\left(F_1^2 - \frac{\kappa^2 q^2}{4M^2}F_2^2\right)\cos^2\frac{\theta}{2} - \frac{q^2}{2M^2}(F_1 + \kappa F_2)^2\sin^2\frac{\theta}{2}\right\}$$

θ Electron scattering angle

κ Anomalous magnetic moment

M Nucleon mass

Sachs Form Factors

- Electric Form Factor: $G_E = F_1 - \tau\kappa F_2$
- Magnetic Form Factor: $G_M = F_1 + \kappa F_2$

$$\tau = \frac{-q^2}{4M^2} = \frac{Q^2}{4M^2}$$

$$\left(\frac{d\sigma}{d\Omega}\right)_{\mathrm{Lab}} = \left(\frac{d\sigma}{d\Omega}\right)_{\mathrm{Mott}} \left[\frac{G_E^2 + \tau\, G_M^2}{1+\tau} + 2\,\tau\, G_M^2 \tan^2\frac{\theta_e}{2}\right]$$

where $$\left(\frac{d\sigma}{d\Omega}\right)_{\mathrm{Mott}} = \frac{\alpha^2}{4E_e^2 \sin^4(\theta_e/2)}\,\frac{E_e^{'}}{E_e}\cos^2(\theta_e/2)$$

Rosenbluth Separation Technique

$$\left(\frac{d\sigma}{d\Omega}\right)_{\text{Lab}} = \left(\frac{d\sigma}{d\Omega}\right)_{\text{Mott}} \left[\frac{G_E^2 + \tau\, G_M^2}{1+\tau} + 2\,\tau\, G_M^2 \tan^2\frac{\theta_e}{2}\right]$$

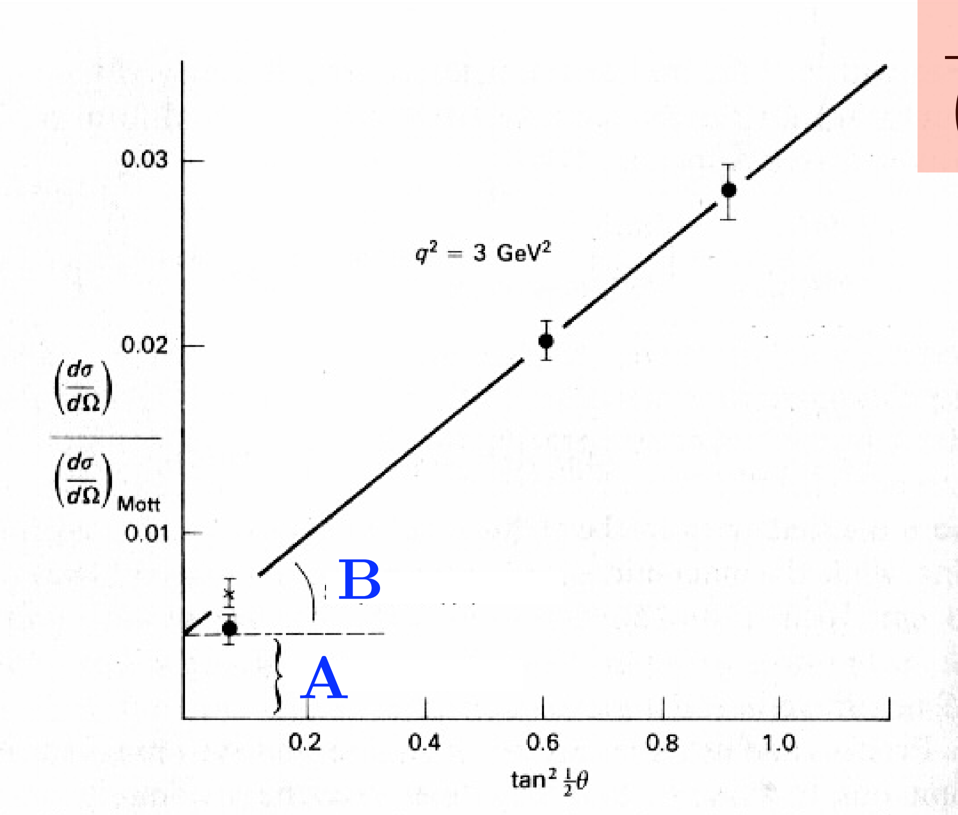

$$\frac{\left(\frac{d\sigma}{d\Omega}\right)_{\text{Lab}}}{\left(\frac{d\sigma}{d\Omega}\right)_{\text{Mott}}} = A + B\tan^2(\theta_e/2)$$

$$A \equiv \frac{G_E^2 + \tau\, G_M^2}{1+\tau}$$ **(Intercept)**

$$B \equiv 2\tau\, G_M^2$$ **(Slope)**

$$Q^2 = 4E_e E_e' \sin^2(\theta_e/2)$$

Limited accuracy at large Q^2

$$G_{En}^2(Q^2) \ll \tau\, G_{Mn}^2(Q^2)$$

Rosenbluth Separation Technique (cont)

Inclusive electron-deuteron quasielastic scattering

- $(G_E^n)^2$ was extracted from the quasielastic ed cross section measurements (unpolarized beam and target)

- Measurements of G_E^n and G_M^n using Rosenbluth separation technique.

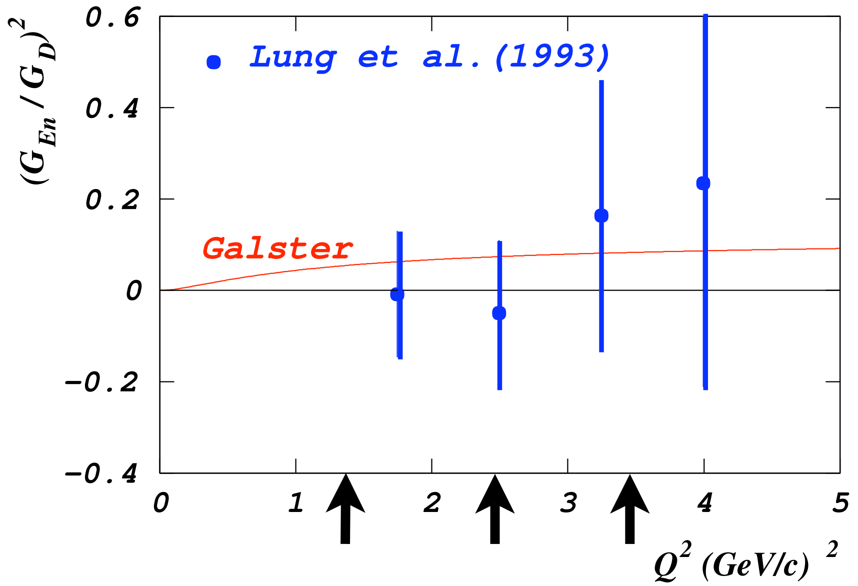

A. Lung et al.,
Phys. Rev. Lett. **70** (1993) 718

Results are consistent with the Galster parameterization and $G_E^n = 0$

G_{En} from deuteron A(Q)

- G_E^n extracted from the deuteron structure function data A(Q) in elastic ed scattering (unpolarized electron and target)
- Large systematic uncertainties due to model dependence on the deuteron wave function, and removal of the proton contribution

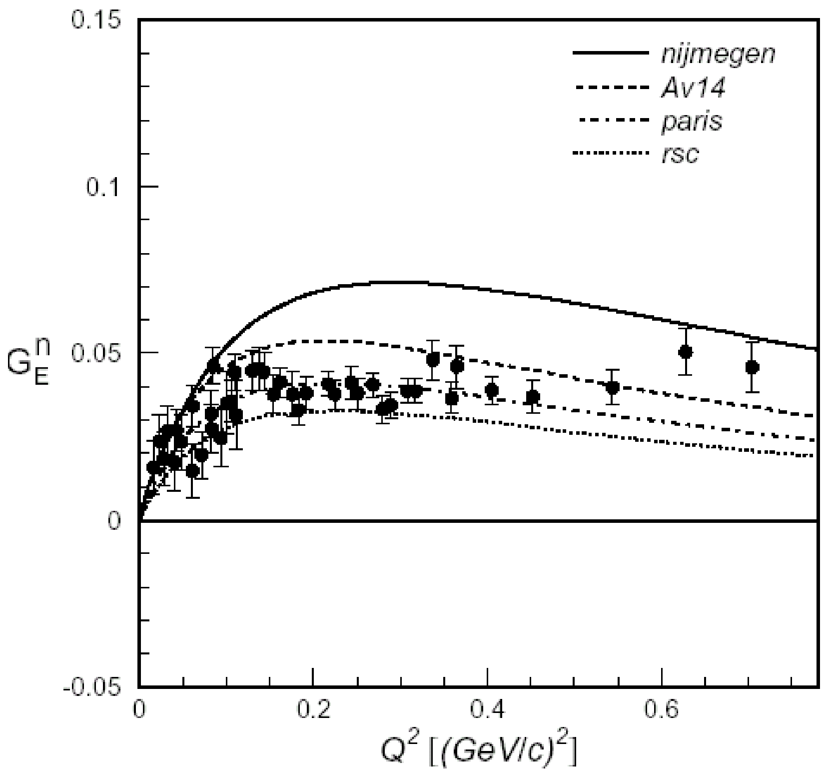

S. Platchkov et al.,
Nucl. Phys. **A510** (1990) 740
(^{1}H(e,e') and ^{2}H(e,e')
A(Q^2) measurements done at the Saclay linear electron accelerator)

S. Galster et al., Nucl. Phys. **B32** (1971)

Galster Parameterization: $(Q^2 < 0.6(\mathrm{GeV/c})^2)$

$$G_E^n = \frac{-\mu_n \tau}{1 + 5.6\tau} G_D$$

$$G_D = \frac{1}{(1 + Q^2/0.71)^2}$$ (Dipole form factor)

Recoil Polarization Technique

- Measurements of $g = G_E^n / G_M^n$ via recoil polarimetry [Akhiezer and Rekalo (1973); Arnold, Carlson, and Gross (1981)]
- Electron Scattering assuming free neutron target: $\vec{e} + n \longrightarrow e' + \vec{n}$
- Electron polarization P_e, is transfered to neutron: sideways component, P_S', longitudinal component P_L',

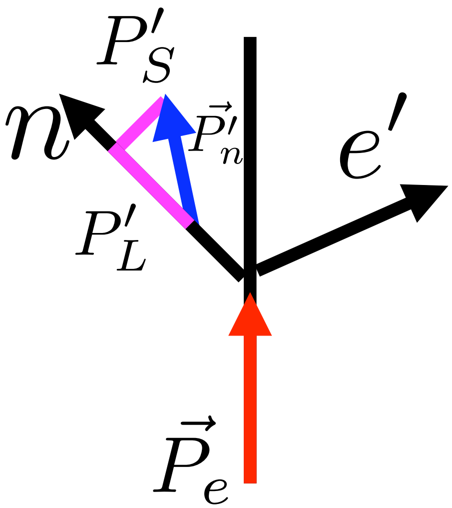

$$I_0 \frac{P_S'}{P_e} = -K_S \, G_M^n \, G_E^n$$

$$I_0 \frac{P_L'}{P_e} = K_L \, (G_M^n)^2$$

$I_0 = (G_E^n)^2 + K_0 \, (G_M^n)^2$; $K_L, K_S,$ and K_0 are kinematic factors.

$$\frac{P_S'}{P_L'} = -\left(\frac{K_S}{K_L}\right)\left(\frac{G_E^n}{G_M^n}\right)$$

(P_e cancels out !!!)

T. Eden et al., Phys. Rev. C**50** (1994) R1749
C. Herberg et al., Eur. Phys. J. A**5** (1999) 131
R. Madey et al., Phys. Rev. Letter 91 122002 (2003)

Recoil Polarization Technique(cont)

Scattering asymmetry from the transverse component of the polarization is measured via a secondary *np* scattering in a polarimeter

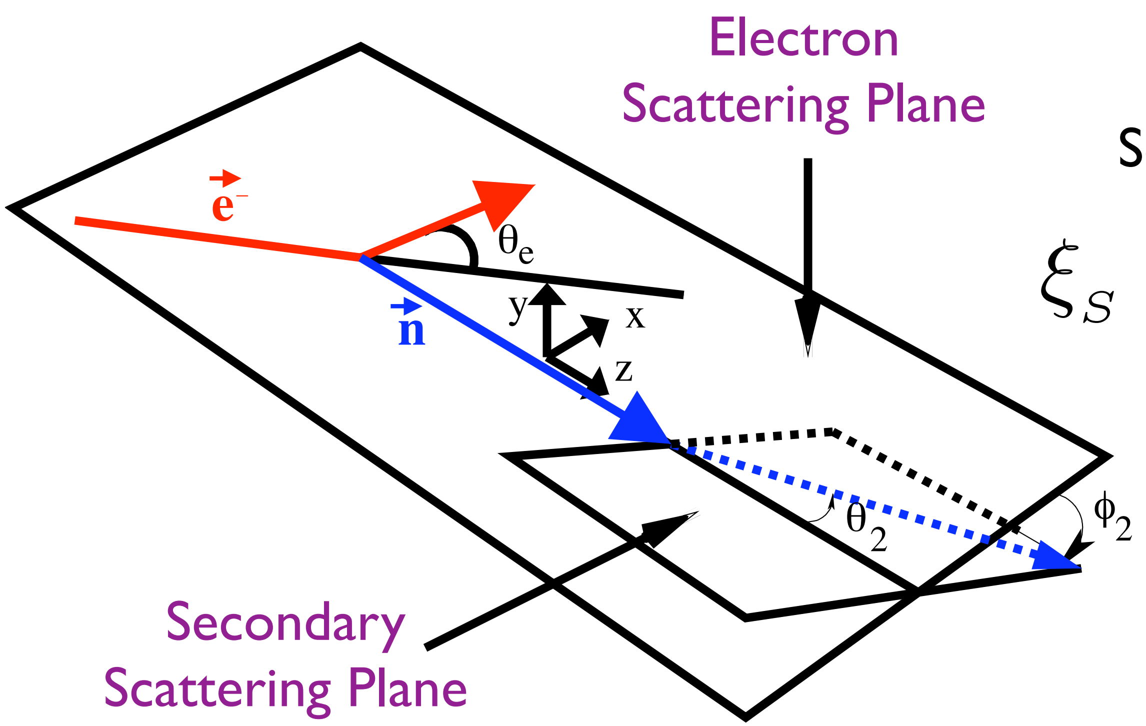

Scattering Asymmetry:

$$\xi_S = P_S^{'} \langle A_y \sin\phi_2 \rangle$$

Experimental Setup (E93038) $d(\vec{e}, e'\vec{n})$

Q^2 =0.45,1.13, 1.45 $(GeV/c)^2$

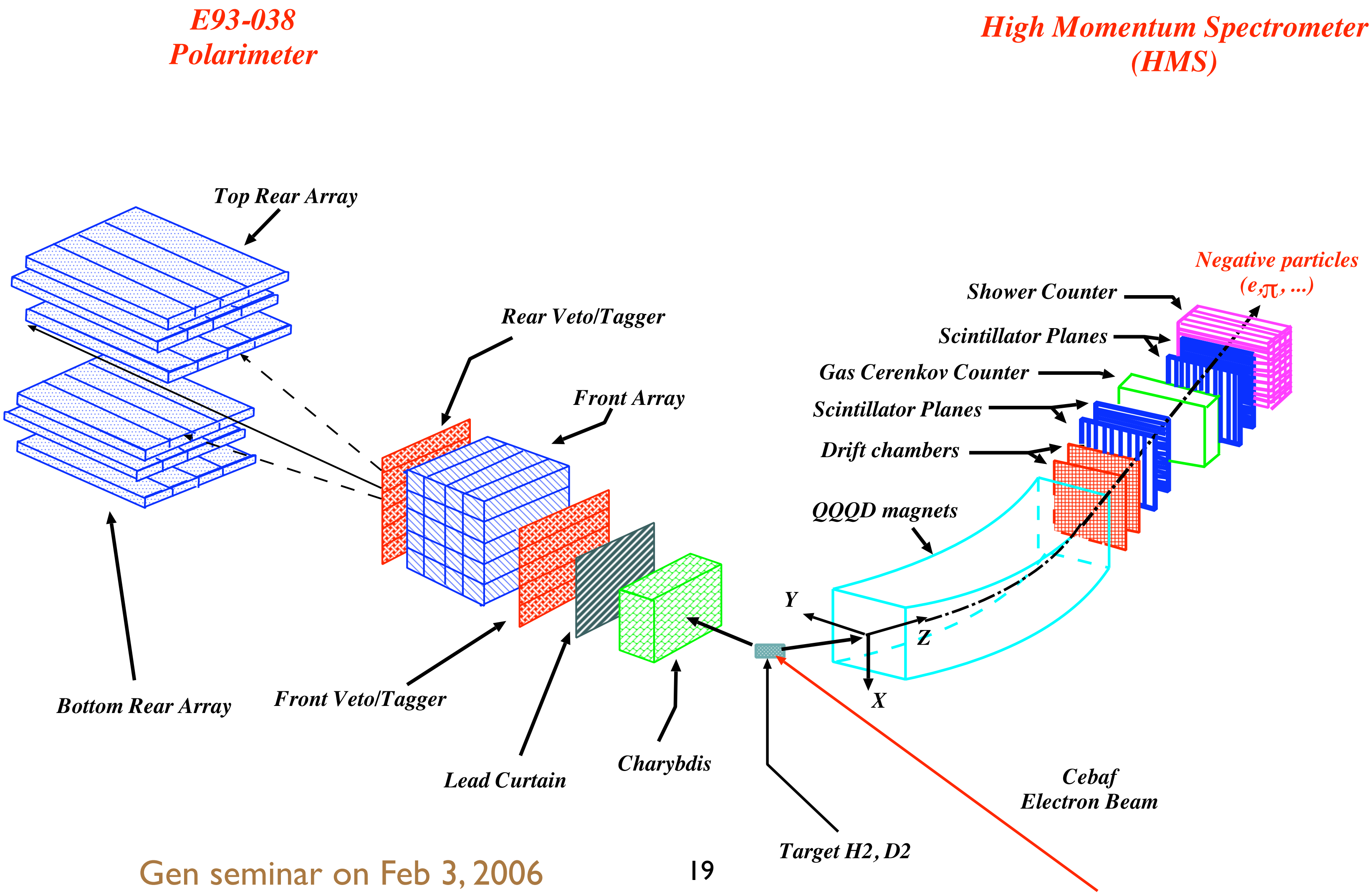

Neutron Polarimeter (E93-038) $d(\vec{e}, e'\vec{n})$

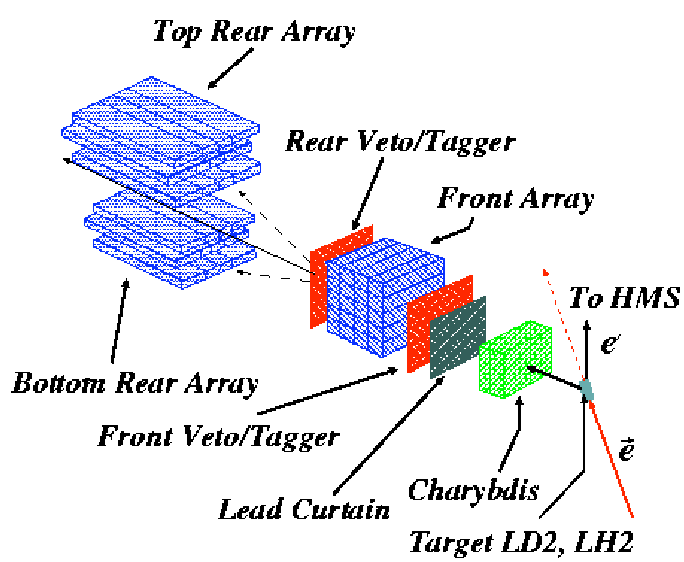

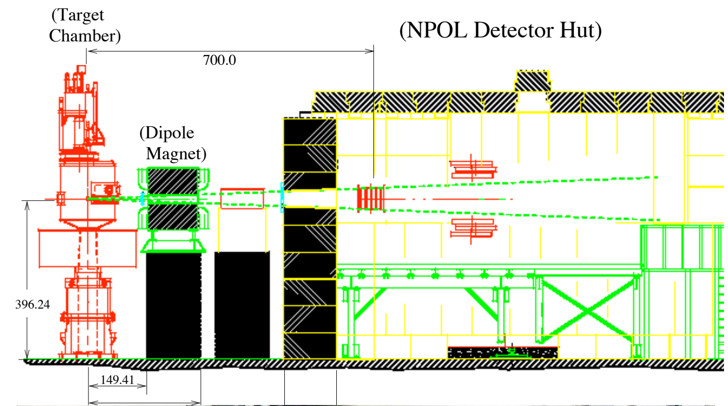

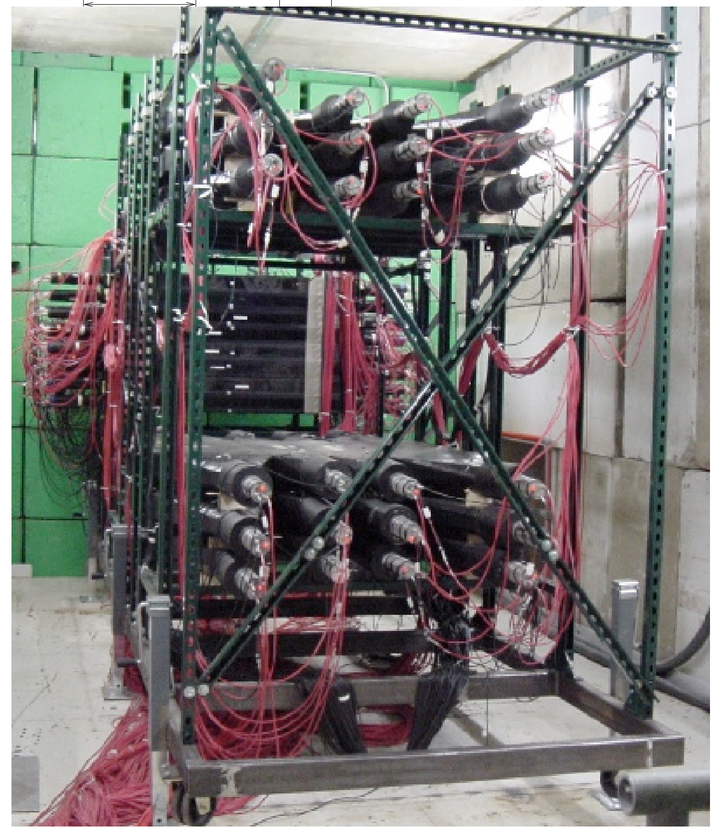

- Front, Rear, and Veto arrays
- Measure scattering asymmetries
- 10-cm Lead: Reduce Background
- Charybdis (Dipole Magnet) Precesses the Neutron Polarization
- Measure TOF and Energy Deposited
- NPOL Heavily Shielded

Time-of-Flight (TOF) Spectra in Front and Rear (Neutral Events)

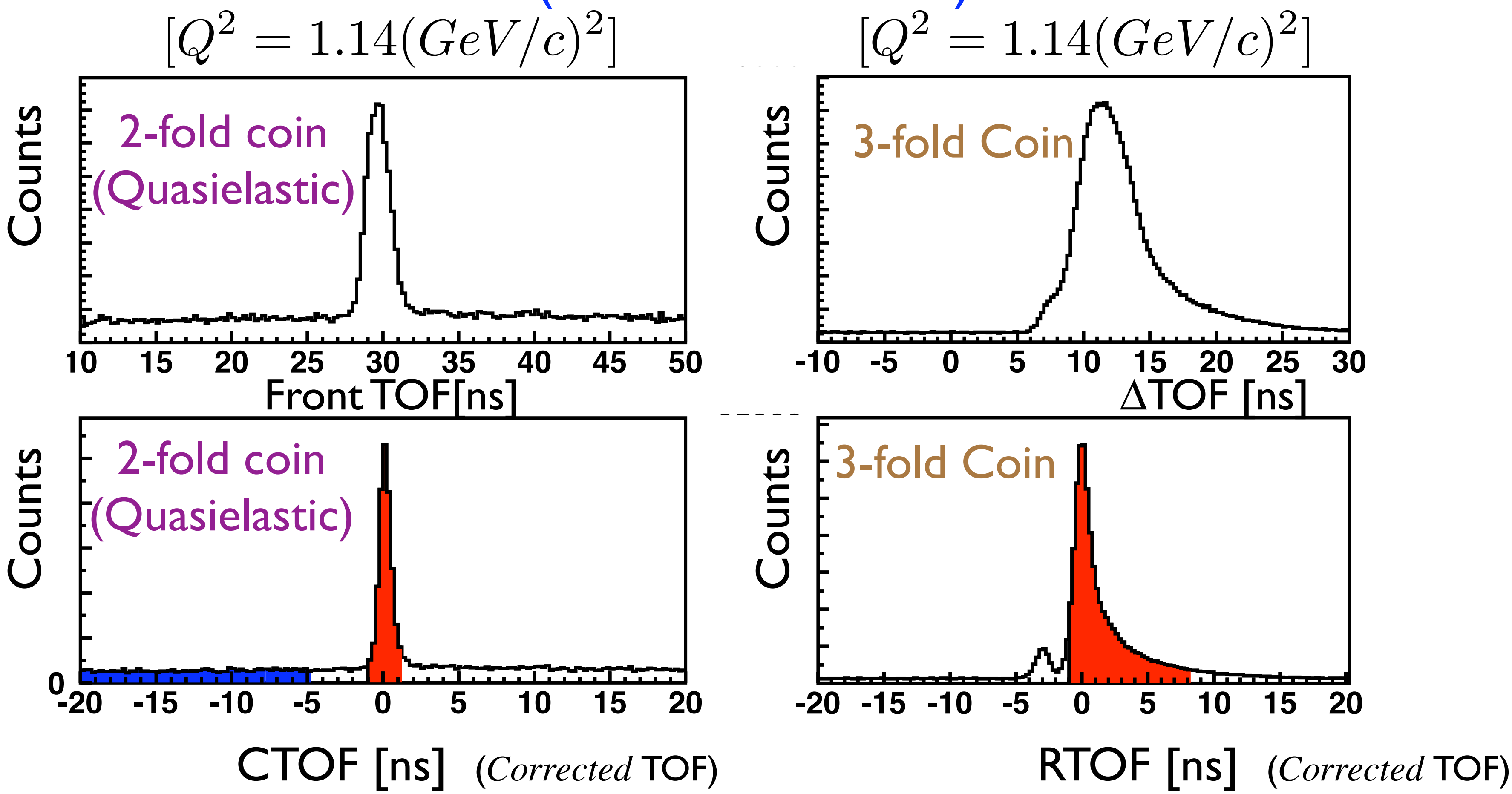

- ΔTOF = RearTOF – FrontTOF
- *Corrected* TOF = [*Measured* TOF] – [*Predicted* TOF]

Polarized Target Technique

- G^n_E was extracted from quasielastic $(\vec{e}, e'n)$ reaction using longitudinally polarized electron beam and a polarized target (^{2}H or ^{3}He)
- The Beam-Target asymmetry A is given by:

$$A = P_e P_n f \frac{a \sin\Theta \cos\varphi\, G_E^n G_M^n + b \cos\Theta\, (G_M^n)^2}{c\,(G_E^n)^2 + d\,(G_M^n)^2} = A_\perp \sin\Theta \cos\varphi + A_\parallel \cos\Theta$$

$$[A_\perp = A(\Theta = 90^\circ, \phi = 0^\circ),\ A_\parallel = A(\Theta = 0^\circ, \phi = 0^\circ)]$$

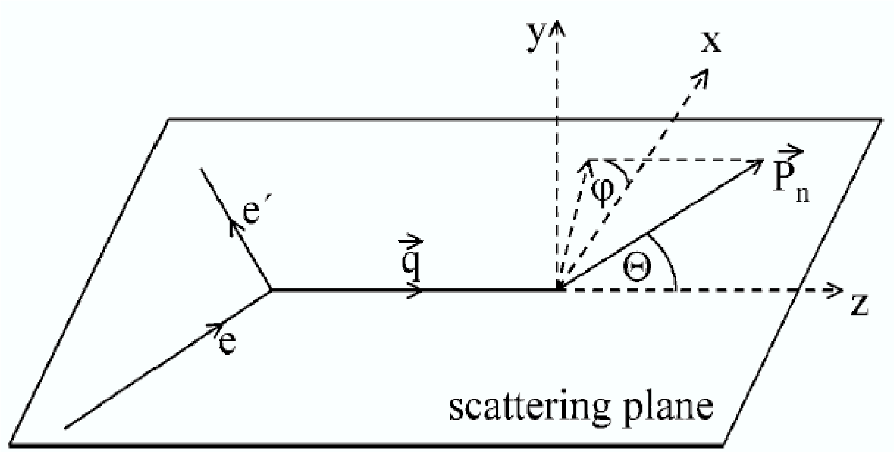

Target Polarization angles

(i) G^n_E from measurements of $A_\perp$:

JLab, NIKHEF: $\vec{d}(\vec{e}, e'n)$

JLab Hall A: $^3\vec{\mathrm{He}}(\vec{e}, e'n)$

(ii) G^n_E from the ratio of two asymmetries,

$$\frac{A_\perp}{A_\parallel} = \frac{a}{b} \frac{G_E^n}{G_M^n}$$

(Reduce systematic errors)

Mainz A1, Mainz A3: $^3\vec{\mathrm{He}}(\vec{e}, e'n)$

E93-026 Experiment $\vec{d}(\vec{e}, e'n)$

$Q^2 = 0.5, 1.0\ (\text{GeV}/c)^2$

Target polarization is perpendicular to $\vec{q}$

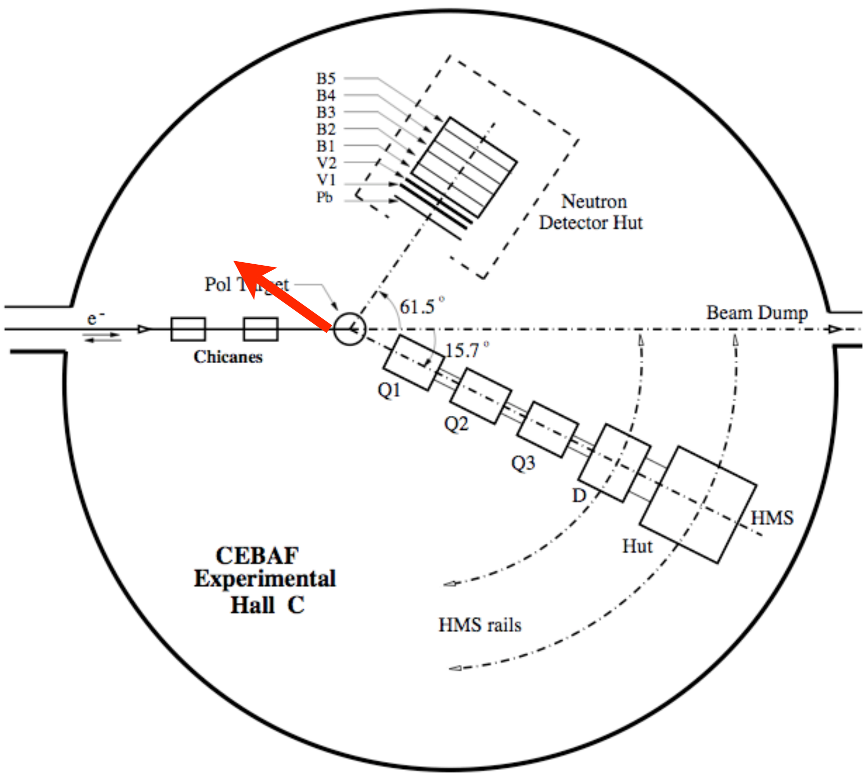

Figure 6.1: Equipment on Hall C floor during E93-026 experiment.

Neutron Detectors (side view)

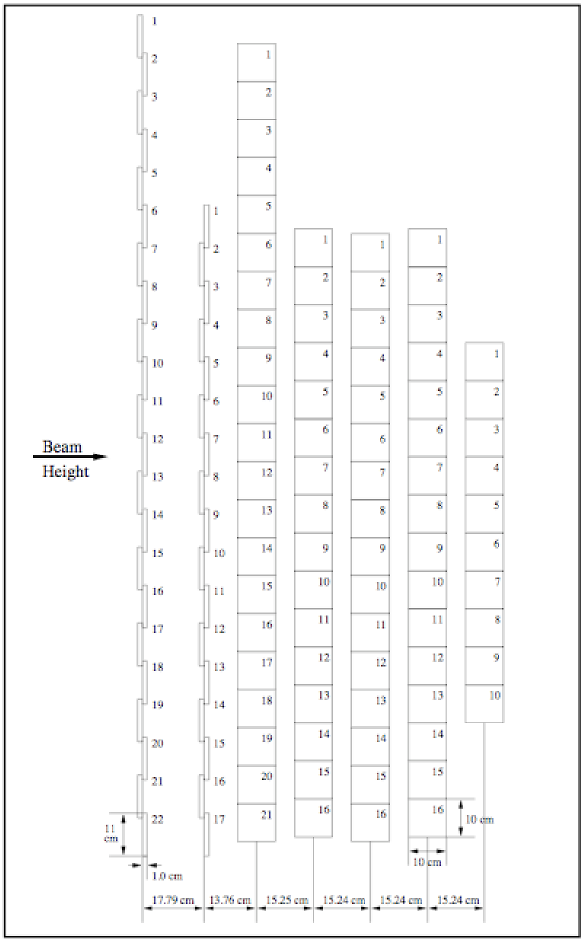

Figure 6.35: Side view of the E93-026 neutron detector configuration.

E93-026 Experiment $\vec{d}(\vec{e}, e'n)$

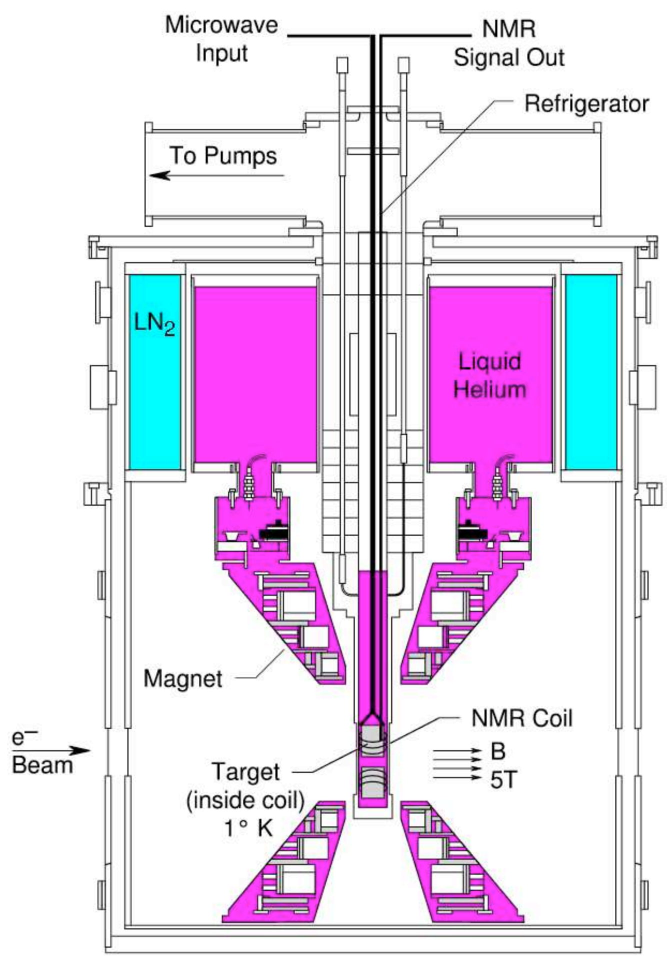

Polarized Target (side view)

- Target Ladder
  Two ND_3 cups
  One Carbon disc (7mm thick)
- 5-Tesla Target Field
- Target Polarization ~21%
- Beam current ~100nA

E02-013 Experiment $^3\vec{He}(\vec{e},e'n)$

Will start running in 3 weeks in Hall A !!

- Precise measurements of G_{En} at high Q^2 (=1.3, 2.4, 3.4 (GeV/c)^2)

Three main components:

- Polarized 3He Target
- BigBite Detector
- Neutron Detector

E02-013 Experiment $^3\vec{H}e(\vec{e},e'n)$

^{3}He as an Effective Neutron Target

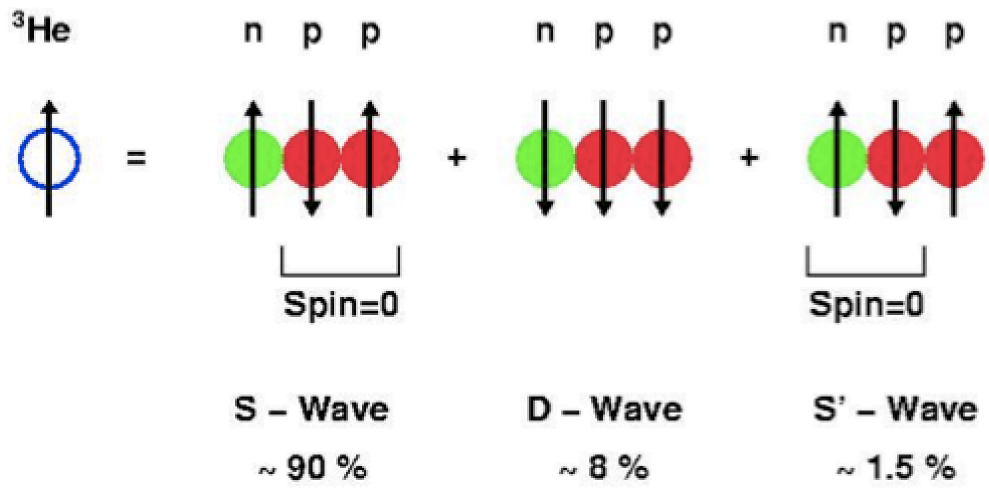

- Naïve picture:
  - neutron carries the spin of ^{3}He, protons are unpolarized
- Actual calculations:
  - neutron polarization ~86%; proton polarization ~-2.8%
  - further medium effects: reduction of cross section (reproduced by Glauber approximation type calculations e.g.)

E02-013 Experiment $^3\vec{H}e(\vec{e},e'n)$

The Hall A Polarized Helium-3 Target

- Principle: spin exchange between optically pumped alkali-metal vapor and ^{3}He
- High pressure cell (10 atm), cell length 40 cm
- Target polarization 40%
- Beam current: up to 15μA
- Luminosity 1.0*10^{36} e-neutron/s/cm^2

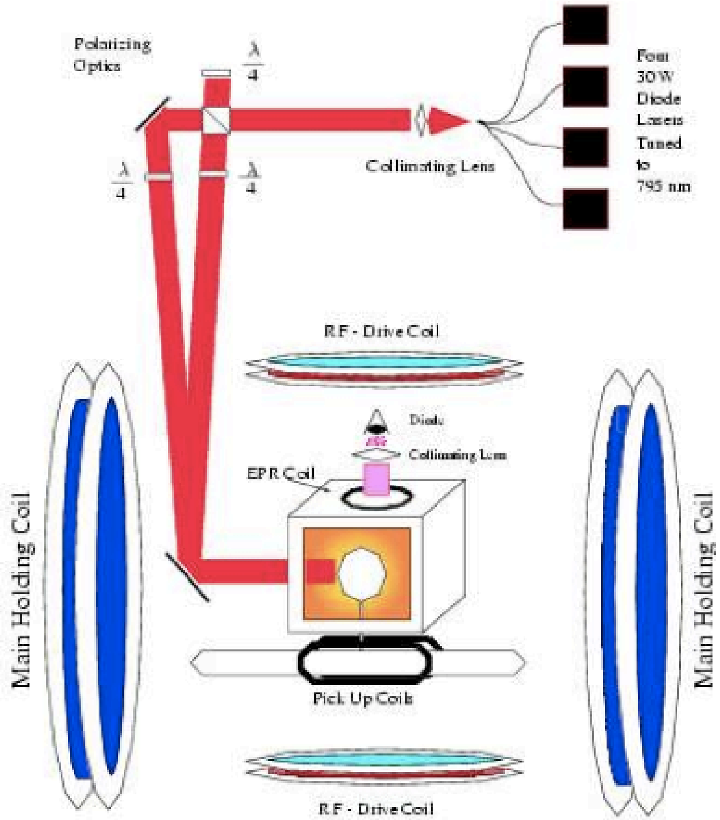

E02-013 Experiment $^3\vec{H}e(\vec{e}, e'n)$

BigBite Detector

- Non-focusing, large acceptance(76msr) detector
- dP/P=1-1.5% at 1.2T field energy resolution ~ 50MeV
- Drift Chambers, Shower Counter, Trigger scintillators

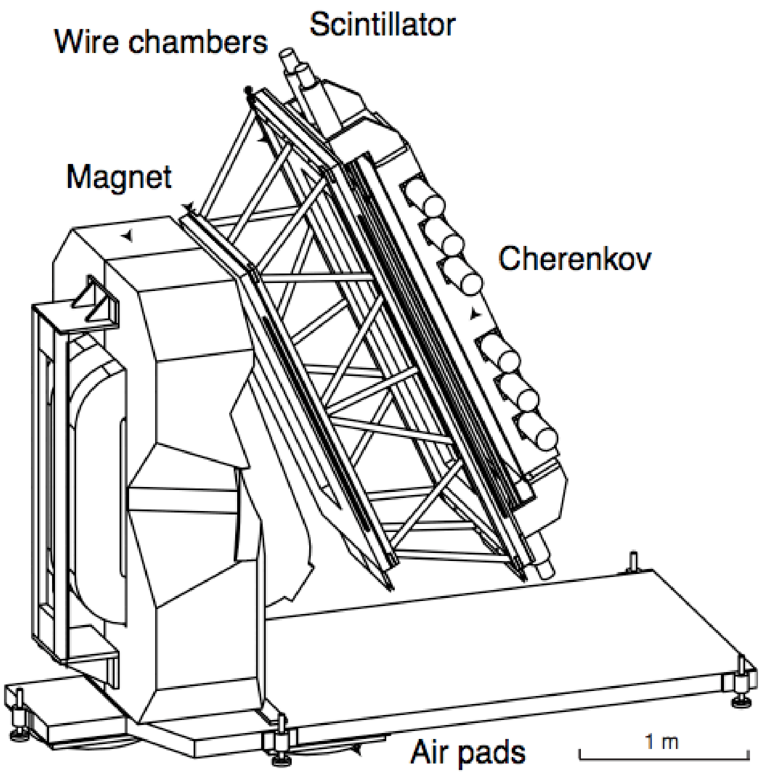

E02-013 Experiment $^{3}\vec{H}e(\vec{e},e'n)$

Neutron Detector

- Lead shielding, Veto(2 layers), ND (5 or 7 Layers)
- Scintilators with different sizes:
  - $10 \times 10 \times 160\ cm^3$
  - $10 \times 20 \times 180\ cm^3$
  - $10 \times 25 \times 100\ cm^3$
- High neutron detection efficiency (~60% at 2.6GeV/c)
- Measure neutron TOF, detection position, and pulse-height energy.
- Designed to match the large BigBite acceptance
- Detect high momentum neutrons (=high velocity)

Summary

- Double polarization techniques are necessary to perform precise measurements of G_{En} / G_{Mn}
- E02-013 G_{En} measurements at Q^2 =2.4 and 3.4 $(GeV/c)^2$ will be the first precise data at Q^2 >2 $(GeV/c)^2$.
- G_{En} at Q^2 =4.3 $(GeV/c)^2$ will be measured in Hall C in the future (approved) using recoil polarization technique.

References

- Gen Papers:
  http://hallaweb.jlab.org/experiment/E02-013/pubs.html
- Gen Theses (Hall C)
  - Hongguo Zhu (E93-026; **d**(**e**,e'n)p)
  - Brad Plaster (E93-038; d(**e,**e'**n**)p)
  - Shigeyuki Tajima (E93-038; d(**e,**e'**n**)p)
- To learn about polarized 3He target, read Hall A theses:
  - Xiaochao Zheng (A1n)
  - Karl Slifer (GDH)

Comparison of Data with Theoretical Models

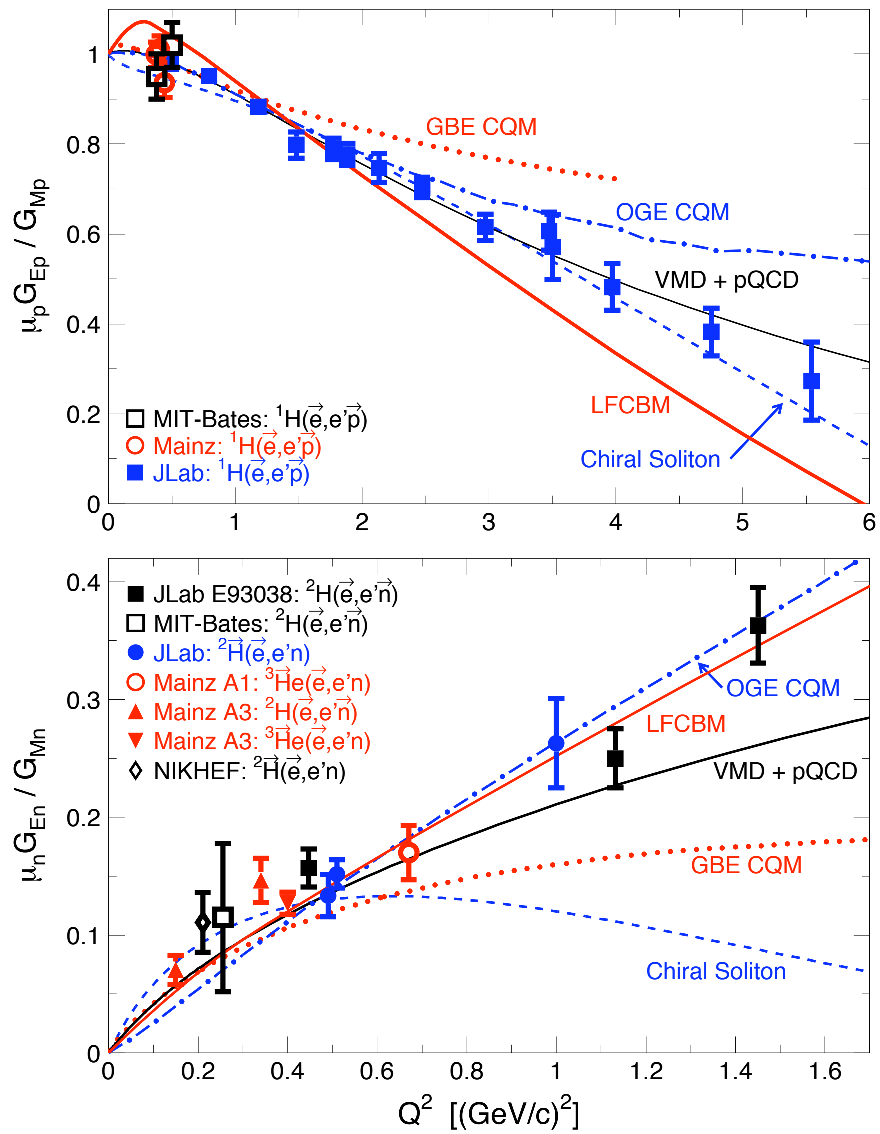

- Chiral Soliton: Holzwarth (1996,2002)
- CQM with GBE: Wagenbrunn et al. (2001), Boffi et al.(2002)
- Light Front Cloudy Bag Model (LFCBM) Miller (2002)
- Light Front CQM with OGE: Cardarelli and Simula (2000) and Simula (2001)
- VMD+pQCD: Lomon (2001,2002)

No model is consistent with both proton and neutron form factor data.

Previous Measurements of G_E^n (III)

G_{En} from Deuteron Quadrupole Form Factor Data

R. Schiavilla and I. Sick, Phys. Rev. C64, 04002(R) (2001)

- Analyzed world data for $G_Q(Q^2)$, the deuteron quadruple form factor
- ~340 data points from ed elastic scattering
- π-exchange operator contribution to $G_Q(Q^2)$ is dominant up to $Q^2 \sim 1.7\ (\mathrm{GeV/c})^2$, leading to reasonable systematic errors.
- Error bars include both theoretical and statistical errors.